Bio-directed synthesis and assembly of nanomaterials

Wendy J. Crookes-Goodson, Joseph M. Slocik and Rajesh R. Naik*

Received 8th May 2008
First published as an Advance Article on the web 26th September 2008
DOI: 10.1039/b702825n

This *tutorial review* provides an overview of bio-directed synthesis of nanomaterials, starting with the foundation of biomineralization research—how organisms are able to biomineralize materials *in vivo*—and progressing to studies of biomineralization *in vitro*. This research is of interest to biologists, chemists and materials scientists alike, especially in light of efforts to find 'greener' methods of inorganic material synthesis. Examples of applications of nanomaterials synthesized by these methods are provided to demonstrate the end goals of biomineralization research.

1.0. Introduction

The synthesis of nanomaterials such as silica, metals and metal alloys by biological molecules is known as biomineralization.[1] Over millions of years of evolution, nature has evolved mechanisms to produce such nanomaterials for a wide variety of purposes. Diatoms produce exquisitely intricate silica shells with nanoscaled spikes, pores and valleys[2,3] and sponges produce spicules[4] that are utilized for structure and protection. Bacteria synthesize crystalline magnetic nanoparticles for navigation and orientation.[5,6] Algae, plants and bacteria produce metal nanoparticles as a consequence of detoxification pathways.[7] In many cases, the nanomaterials are produced under genetic control, resulting in specific morphologies, sizes and crystallinities of the structures and particles.[4] Remarkably, all of this synthesis and assembly occurs under ambient conditions. This is in sharp contrast to the caustic reagents and high temperatures and pressures that are utilized for industrial synthesis of the same materials. As well, often industry cannot achieve the nanoscale size features that nature produces routinely. Thus, researchers have looked towards natural systems for ways to produce nanoparticles by 'green chemistry'.[7] They have utilized the biomolecules (or parts of them) that organisms use, as well as used nature to inspire the design of new biomolecules that have proven able to replicate nature's ability to synthesize nanoparticles.[1,7] This review will encompass various aspects of biomineralization, from classical examples of silica and metal deposition in organisms to *in vitro* systems that utilize bio-inspired molecules to synthesize nanoparticles. We will also discuss the applications of biomimetically-produced nanomaterials.

Materials and Manufacturing Directorate, Air Force Research Laboratory, Wright-Patterson AFB, Dayton, OH, USA. E-mail: rajesh.naik@wpafb.af.mil; Fax: 937-255-9157; Tel: 937-255-9717

2.0. Synthesis of inorganic materials by organisms

2.1 Biomineralization of silica by diatoms

Silicon dioxide is a critical component of micro- and nanodevices and is utilized in the production of sensors, actuators and other devices for the telecommunications, computing and optics industries. Currently, production of silicon dioxide for industry is accomplished through the Stöber method under extreme pH or flame hydrolysis of $SiCl_4$ and H_2O which requires high temperatures and pressures. In contrast, diatoms, sponges and plants annually produce 6.7 gigatons of hydrated SiO_2, or biosilica, under ambient conditions.

Diatoms are unicellular eukaryotic organisms that populate the world's fresh- and saltwater ecosystems. One of the most remarkable aspects of diatoms is their range of intricate morphologies (Fig. 1A and B), rooted in their elaborate silica cell walls. The cell walls, known as a frustules, are composed of two halves (thecae) that fit together like a Petri dish.[3] The top and bottom surfaces of the thecae, termed valves, often have an array of pores and branches composed of nanostuctured granular silica (Fig. 1C). The positioning and size of the pores and branches are species-specific, and therefore, genetically determined.[2] Remarkably, these features are

Wendy Crookes-Goodson is a molecular biologist in the Nanostructured and Biological Materials Branch, Materials and Manufacturing Directorate, Air Force Research Laboratory, Wright-Patterson Air Force Base, Dayton, Ohio. She received her PhD in Biology from the University of Michigan in 2000. She joined AFRL in 2005 to assist in directing bio-based projects in the Biotechnology Group.

Joseph Slocik is a research scientist in the Nanostructured and Biological Materials Branch, Materials and Manufacturing Directorate, AFRL, Wright-Patterson AFB, Dayton, Ohio. He received his PhD in Chemistry from Vanderbilt University in 2004. His projects currently involve biomimetic synthesis, bio-derived catalysts, and peptide mediated assembly.

Rajesh Naik is Biotechnology Technical Advisor of the Nanostructured and Biological Materials Branch, Materials and Manufacturing Directorate, AFRL, Wright-Patterson AFB, Dayton, Ohio. He received his PhD in Cellular/Molecular Biology in 1998 from Carnegie Mellon University in Pittsburgh. He joined AFRL as a research scientist in 1999.

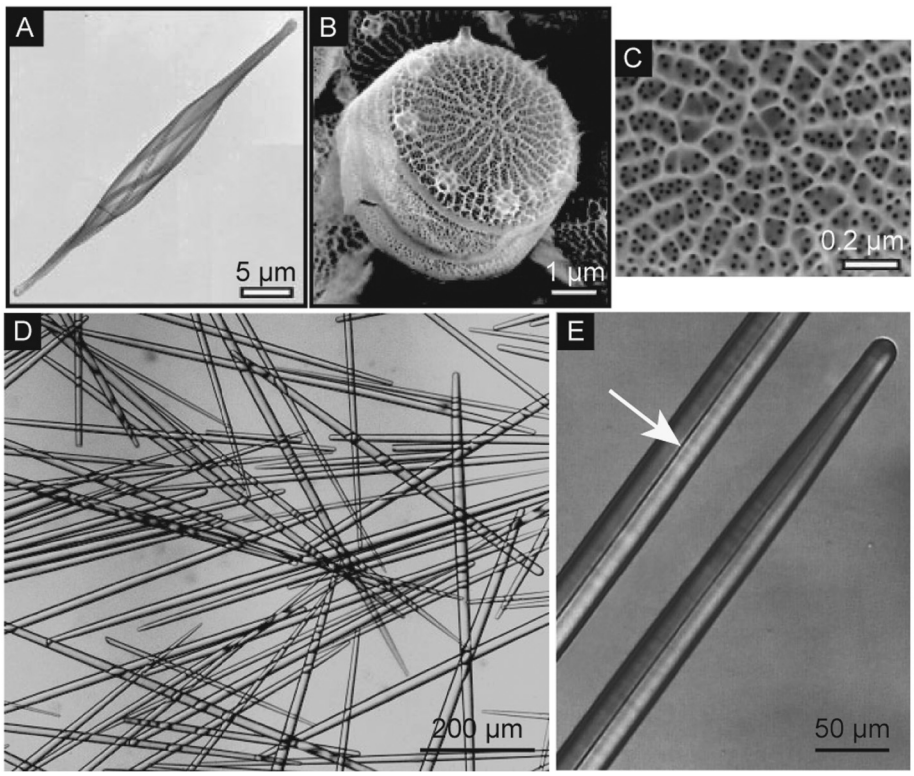

Fig. 1 Structures of diatom and sponge silica. (A) Structure of the cell wall of the pennate diatom *Cylindrotheca fusiformis*. (B) Structure of the cell wall of centric diatom *Thalassiosira pseudonana*. (C) Higher magnification image of *T. pseudonana* cell wall. (D) Isolated spicules from the sponge *Tethya aurantia*. (E) Higher magnification image showing axial filaments running through the center of the *T. aurantia* spicules (arrow). Panels A, B and C were reprinted in part from N. Poulsen and N. Kroger, *J. Biol. Chem.*, 2004, **279**, 42993–42999. Copyright 2004, The American Society for Biochemistry and Molecular Biology. Panels D and E were reprinted from *Microscopy Res. Tech.*, 2003, **62**(4), 356–367. Copyright © 2003, Wiley-Liss, Inc. Reprinted with permission of Wiley-Liss, Inc., a subsidiary of John Wiley & Sons, Inc.

synthesized on a scale much smaller, and in a more controlled manner, than humans are capable of producing synthetically. Thus, the methods by which these features arise are of great interest to biologists and materials scientists alike.

Creation of new thecae occurs in a specialized vesicle, the silica deposition vesicle (SDV) in which two critical types of molecules reside: silaffins and long-chain polyamines (LCPAs).[2,3,8] Both are tightly associated with silica and difficult to extract; current methods involve either dissolving the silica with anhydrous hydrofluoric acid or with acidified ammonium fluoride.[2] *In vitro* studies suggest that, in most diatoms, silica biomineralization occurs through the concerted activity of these molecules.

Silaffins are rich in hydroxyamino acids and lysines and are highly post-translationally modified through phosphorylation, sulfation, glycosylation and/or alkylation. There appears to be little sequence homology among silaffins from different species, but the chemical compositions are similar. Roles of individual silaffins are only known through *in vitro* silica precipitation studies. While some (*e.g.*, natSil-1A from *Cylindrotheca fusiformis*) are capable of precipitating silica alone, others (*e.g.*, natSil-2 from *C. fusiformis* and tpSil-1H, -1L, -2H, -2L and -3 from *Thalassiosira pseudonana*) appear to be regulatory and depend on the presence of other silaffins or LCPA.[2,8]

LCPAs also precipitate silicic acid *in vitro* and may be critical components of cell wall synthesis *in vivo*. Most LCPAs characterized to date are repeats of N-methylated oligopropyleneimine with terminal putrescine or putrescine derivatives. Some, however, are composed of oligo-propyleneimines attached to a propylamine, spermine, or spermidine basis.[2] There has been some suggestion that chain length and degree of methylation are species-specific, but the recent finding that *T. pseudonana* contains at least two types of LCPA molecules calls this hypothesis into question.[2] Regardless, the contribution of these structural variations to resulting silica morphologies is not currently understood.

Together, silaffins and LCPAs form supramolecular assemblies that are capable of precipitating silica. *In vitro*, the particular silaffin–LCPA mixture that is utilized determines the morphology of the resulting silica, from spheres to sheets to plates.[2,8] Poulsen and Kröger hypothesize that silica morphology is dictated by the silaffins, as opposed to the LCPAs. Polycondensation of silicic acid probably relies on hydrogen bonding between the amino groups of the polyamines in both the silaffins and LCPAs and Si–OH groups of silicic acid.[8] The hydroxyl groups present in silaffins may form hydrogen bonds with the LCPAs, preventing the LCPAs from interacting with silicic acid and inhibiting polymerization. Thus, the relative abundance of hydroxyl groups in the silaffins present in the SDV may regulate LCPA-dependent silica formation.

While Poulsen and Kröger hypothesize that silaffins determine silica morphology on the microscale, Hildebrand and

colleagues suggest that LCPAs may be a key component to determining the macroscale structure of the valve.[9] In an expression study designed to identify cDNAs involved in specific stages of cell wall synthesis, they observed upregulation of ornithine decarboxylase, ornithine carbamoyltransferase and *S*-adenosylmethionine decarboxylase, enzymes of the polyamine synthesis pathway.[9] Treatment of diatom cells with 1,3-diaminopropane dihydrochloride, an inhibitor of ornithine decarboxylase, resulted in aberrant valve formation. The cells appeared inhibited in the later stages of valve formation, causing the authors to speculate that the role of LCPAs in cell wall synthesis is in the thickening of the valves to form the final structure.

2.2 Silicification by sponges

Like diatoms, sponges (phylum Porifera), the oldest metazoan organisms, produce a variety of intricate skeletal elements that currently cannot be duplicated in the laboratory or by industry.[4,10] They are classified into three classes: Hexactinellida, Desmospongiae and Calcarea. Although all three utilize biomineralization in forming their skeletons, only the Hexactinellida and Desmospongiae do so through deposition of silica while Calcerea utilize calcium carbonate instead and will not be discussed here.[11] Sponges take advantage of high levels of environmental silicon to build robust structures of amorphous silica ($SiO_2{\cdot}nH_2O$). These structures, called spicules, range from 1 μm to 3 m in length and microns to millimeters in diameter, exhibit a low elastic modulus and high fracture toughness (Fig. 1D).[12] They are used for structure, defense, food entrapment, and anchoring to substrates.[13] Spicule synthesis and morphology are genetically determined but are also influenced by environmental factors such as wave forces and levels of silicon.[13]

Spicules are composed of annular layers of nanoparticulate silica (particle diameter of $\sim$70 nm) surrounding a central proteinaceous axial filament, which not only templates silica deposition but also catalyzes the hydrolysis of silicon alkoxides (Fig. 1E).[4] Axial filaments are composed predominantly of three proteins, dubbed silicateins α, β and γ,[4] that associate into dimers, tetramers and hexamers.[10] The silicateins undergo phosphorylation,[10] although the contribution of these phosphates to silicatein activity has not yet been explored.

Silicateins α and β (the gene encoding silicatein γ remains uncloned) are highly homologous to cathepsins, cysteine endopeptidases that catalyze peptide bond cleavage through the action of a catalytic triad of amino acids: cysteine, histidine and aspartic acid. However, all known silicateins substitute the cysteine of the triad for serine. Morse and colleagues postulated how silicateins catalyze silicification based on the presence of this conserved substitution and the well-known action of cysteine proteases.[4] They hypothesized that the serine, histidine and asparagine residues provide silicateins with enhanced catalytic activity *via* nucleophilic attack on the Si atom of silicon alkoxide. The nucleophilicity of the oxygen of serine is enhanced by hydrogen bonding between the imidazole nitrogen of histidine and the hydroxyl group of serine. This allows the nucleophilic serine to attack the silicon atom of the first alkoxide bond in silicon ethoxide, forming a protein–O–Si intermediate, and then causing complete hydrolysis of the first alkoxide bond by water. Lastly, the oxygen of Si–OH on the first hydrolyzed silicon ethoxide attacks a second hydrolyzed silicon ethoxide, leading to condensation of the two intermediates. This proposed catalytic mechanism is supported through mutagenesis of the catalytic triad.[4]

While it is clear that silicateins are necessary for spiculogenesis and sufficient for silicification, other proteins may participate. Galectin, a carbohydrate binding protein predominant in extracellular matrices of sponges, was upregulated in the presence of the silica precursor tetraethoxysilane, and localized to both the axial filament and to the outside of spicules in *Suberites domuncula*.[11] Further, galectin co-immunoprecipitated silicateins and enhanced their ability to synthesize silica *in vitro*. Muller and colleagues suggest that galectin could potentially aid in aligning silicatein proteins.

2.3 Magnetic particle formation in bacteria

Another remarkable example of biomineralization is the deposition of magnetic materials in bacteria, algae, termites, bees, molluscs, fish and pigeons.[14,15] These organisms use bio-derived magnetic particles for navigation. Perhaps the best studied are magnetotactic bacteria, which contain magnetic particles (MP) composed of greigite (Fe_3S_4) or magnetite (Fe_3O_4) (Fig. 2A). The majority of magnetotactic bacteria are Gram-negative, α-Proteobacteria of diverse morphologies (cocci, rods, spirillia and multicellular).[14,16] They can be found in sediments from a variety of aqueous environments and, in general, are nitrate-reducing, obligate microaerobes or aerobes.[15] Their metabolic requirement for low oxygen environments probably drove the evolution of magnetotaxis. The ability of magnetotactic bacteria to navigate on geomagnetic lines (*i.e.*, downwards, towards the poles) helps them to migrate towards micro- or anaerobic environments at soil/water interfaces, or just below them.[14] Likewise, mineralization of magnetic particles in magnetotactic bacteria is dependent upon low levels of environmental oxygen; there is a strong negative correlation between environmental oxygen levels and Fe_3O_4 synthesis in *M. gryphiswaldense*.[14]

Magnetotaxis in bacteria is a passive response to the presence of a magnetic field. The bacterium's MPs are packaged in cellular membranes, creating an organelle called a magnetosome. The magnetosomes are arranged in a chain (or chains) that stretches from one cell pole to the other (Fig. 2A and B). This chain is tethered to the cell membrane *via* cytoskeletal filaments that run parallel to the long axis of the cell body (Fig. 2B).[16] Each MP in the chain is a single domain magnetic particle with its own dipole moment; the overall magnetic dipole of the cell is the sum of the individual MP dipoles. When a magnetic force is presented to the cell, the magnetosome aligns itself to the field, rotating the cell along with it and orienting both in the direction of the magnetic field.

The steps involved in MP formation in bacteria are still being elucidated. After examination of cellular iron uptake in magnetotactic bacteria by Mossbauer spectroscopy, Schuler and colleagues generated a model of magnetite formation in *Magnetospirillium gryphiswaldense*.[17] First, the bacteria can

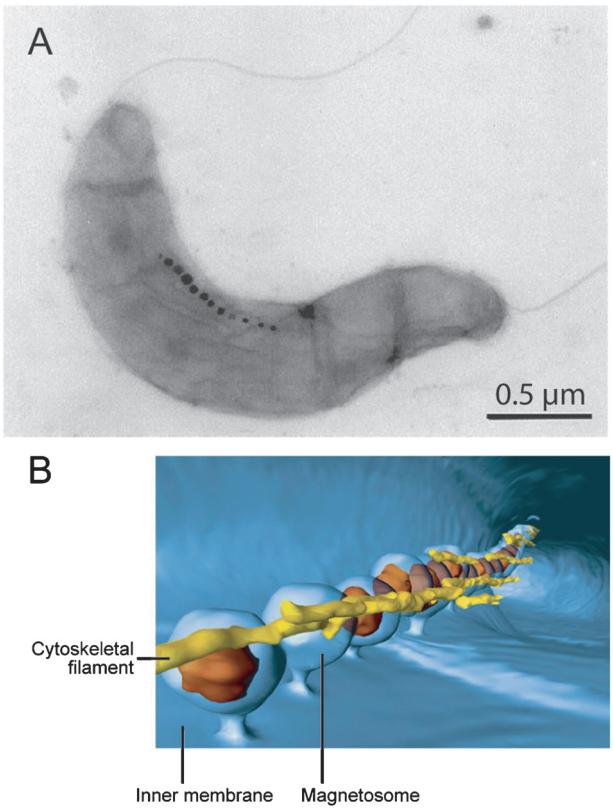

Fig. 2 Magnetosome structure. (A) Electron micrograph of a *Magnetospirillum gryphiswaldense* cell, showing magnetite crystals. (B) Schematic view looking down the long axis of the interior of a *Magnetospirillum magneticum* sp. AMB-1 cell. Magnetosomes are contiguous with the cell membrane and tethered by a cytoskeletal filament. The image was constructed using data obtained by electron cryotomography. Panel A was reprinted with kind permission from Springer Science and Business Media from D. Schuler and R. B. Frankel, Bacterial magnetosomes: microbiology, biomineralization and biotechnological applications (Fig. 1). *Appl. Microbiol. Biotechnol.*, 1999, **52**, 464–473. Copyright 1999. Panel B was reprinted, with permission, from *Annu. Rev. Biochem.*, 2007, **76**, 351–366. Copyright 2007, Annual Reviews www.annualreviews.org.

uptake either ferric iron (Fe^{3+}) or ferrous (Fe^{2+}) iron and convert it intracellularly to a ferrous high spin species.[17] These iron species remain associated with the cytoplasmic membrane until mineralization, when the magnetite crystals are probably released into the magnetosome compartment. Spectral and electrophoretic analysis indicated that membrane-bound ferritin (an iron-storage protein) may play a role, although its exact role has yet to be elucidated. Since no mineral precursors were identified intracellularly, Schuler and colleagues proposed that the next steps of magnetite precipitation occur through fast coprecipitation of ferric and ferrous iron ions at the magnetosome membrane.[17]

Magnetosome proteins may directly participate in this precipitation step. To identify proteins that are directly involved in mineralization, Arakaki *et al.* isolated proteins tightly associated with the MPs.[18] These proteins, Mms5, 6, 7 and 13, all possess a leucine–glycine rich repeating domain (LGLGLGLGAWGPXXLGXXGXAGA). Extensive analysis of Mms6 showed that it contains several regions rich in hydroxyl-containing amino acids, known to possess metal binding capabilities, and hydrophilic domains that could capture metal ions and interact with mineral phases. *In vitro*, recombinant Mms6 bound radiolabelled iron and mineralized 20–30 nm cuboidal magnetic particles, suggesting that it plays a critical role in MP formation *in vivo*.

The size, morphology and crystallinity of the MPs are species-specific. Some species produce between one and hundreds of particles, but most have 15–20, 30–50 nm particles.[16] There may be one or multiple chains of magnetosomes in the cell. The crystal morphologies vary, from rounded to cuboidal to bullet-shaped; all crystal facets ([111], [100] and [110]) are represented.[14] Magnetite particles are generally oriented with their [111] axis along the chain direction, while greigite particles orient with their [100] axis along the chain direction. Despite the wide variety of shapes, sizes and distributions of crystals, within a single bacterial strain there is a remarkably narrow size distribution and in almost all cases the crystals are chemically pure,[14] single-domain magnets with high magnetic coercivity.[16]

Matsunaga and colleagues have capitalized on nature's ability to synthesize these magnetic particles. An advantage of working with bacterial magnetsomes is that the magnetosome membrane remains intact during purification, preventing the particles from agglomerating and also providing a biochemical scaffold upon which can be tethered a variety of labels, proteins, antibodies, *etc.*[15] The purified magnetosomes were used in a variety of applications, including immobilization of enzymes for medical applications, display of G-protein coupled receptors for receptor binding assays, and creation of magnetic cell-separation systems.[15]

2.4 Metal nanoparticle synthesis in bacteria, fungi and plants

While biomineralization of greigite or magnetite has an obvious purpose for magnetotactic bacteria, the production of other metal and metal alloy nanoparticles by organisms is a consequence of detoxification pathways.[7] Metals such as gold, silver and cadmium are present throughout the environment and many are toxic to organisms. For example, they may bind to enzymes of the electron transport chain, which normally coordinate with ions such as magnesium, manganese, zinc or iron, preventing the enzyme from shuttling electrons appropriately and poisoning the respiratory chain. They may also interfere with membrane permeability or with DNA.[19]

Toxic metal ions are taken up nonspecifically through cationic membrane transport systems that normally transport metabolically important cations.[20] Bacteria have evolved mechanisms to counteract this uptake, preventing excessive accumulation of toxic metals. Such mechanisms have been elucidated through the mutagenesis of metal-resistant bacterial strains and subsequent complementation of mutants to identify genes that can restore resistance.[19,20] The mechanisms include enzymatic detoxification/reduction of the metal ions to less toxic metal salts or zero-valent metals, metal-ion efflux systems, and decreases in membrane permeability.[7,19] These can result in intracellular or extracellular complexation and deposition of metal nanoparticles.

Industrial synthesis of Au, Ag and CdS nanoparticles is not environmentally friendly. Synthesis requires harsh reducing agents (*e.g.*, sodium borohydride, hydroxylamine), capping agents (*e.g.*, trioctylphosphine oxide) and organic solvents (*e.g.*, toluene, chloroform);[21] as well as high temperatures and pressures. As in the case of silica biosynthesis, the discovery of metal biomineralization has led various research groups to pursue use of organisms for "green" synthesis of metal nanoparticles under ambient conditions. Researchers have identified many strains of bacteria, fungi, algae and plants that can synthesize metal nanoparticles.[19,21] In most cases, these species/strains were identified by adding silver, gold or cadmium salts to growth media or cell extracts, and monitoring the cells or medium for the presence of nanoparticles. Unfortunately, often the resultant nanoparticles are polydisperse, with variable crystallinities, sizes and morphologies. In addition, it is often unclear which biomolecules are responsible for biomineralization. Biomineralization has been attributed to: reducing sugars (*i.e.*, carbohydrates) attached to cell walls;[22] fatty acids;[23] polyphosphates;[23] hydrogenases;[21] and thiolated peptides such as glutathione.[7] In very few cases have the biomolecules been characterized experimentally. Due to space constraints, this review will focus on selected examples of biomineralization of metal nanoparticles.

The first example is the synthesis of CdS nanoparticles by *E. coli*.[23] CdS nanoparticles are used for biological detection and for creating of optoelectronic transistor components for the semiconductor industry. The properties of CdS nanoparticles can be specifically tuned by altering the size, shape and crystallinity of the particle.[23] There is hope that biology can contribute to this particle tailoring; different biomolecules and biosynthesis systems are being tapped for potential precursor molecules and capping agents. For example, Sweeney *et al.* found that they could grow 2–5 nm CdS (wurtzite) nanoparticles by adding $CdCl_2$ and Na_2S to *E. coli* medium during growth.[23] The growth of the nanoparticles was both strain- and growth-phase dependent; stationary phase cells had an estimated average of $>10\,000$ particles per cell. It is postulated that cellular thiol levels may contribute to the ability of *E. coli* to form CdS nanoparticles intracellularly.

Another example of metal deposition in prokaryotes is the demonstration by Nair and Pradeep that *Lactobacillus* sp., lactic acid-producing bacteria and the active bacterial component of buttermilk, can mineralize silver, gold and gold–silver alloy nanoparticles.[22] To biomineralize silver nanoclusters, $AgNO_3$ and whey were added to the cell media. After >12 h of growth, large colloids formed. The particles ranged from 15–500 nm, but the large particles appeared to be aggregates of smaller particles. The particles were composites with a silver-rich core and organic material at the surface. By using the same *Lactobacillus* sp. and substituting $AgNO_3$ for $HAuCl_4$, gold particles of two sizes distributions (20–50 nm and >100 nm) were deposited inside and outside the cells. These crystals comprised up to 35% of the total cell biomass. Most crystals were hexagonal and X-ray diffraction analysis revealed the [111], [200] and [220] crystal planes.

One final example of metal biosynthesis is the precipitation of gold nanoplates using a cell-free extract from a unicellular green alga, *Chlorella vulgaris*.[21] When Xie *et al.* incubated this extract with $HAuCl_4$ for 48 h, triangular, hexagonal and truncated triangular nanoplates were formed. These plates were crystalline, 0.8–2 μm at their longest edge, and had smooth, well-defined edges. By atomic force microscopy, the plates were measured to be 9–20 nm thick.

The distinct flattened morphology of the crystals suggested that crystal growth was being suppressed on the [111] plane, probably by a capping agent present in the cell extract. To determine which proteins were involved in gold crystal nucleation or capping, Xie *et al.* size-fractionated their algal extract by HPLC. Each fraction was tested for its ability to reduce gold, and positive fractions were further purified. The authors attributed the activity to a 28 kD protein, which they dubbed GSP (gold shape-directing protein). Purified GSP was capable of forming gold nanoparticles and it had a strong influence on gold nanoparticle morphogenesis. Increasing the amount of GSP in a reaction increased the reaction rate but decreased the average lateral size of the nanoplates (from 19 nm to 1.7 nm).[21] In addition, increasing GSP concentrations decreased the nanoplate yield (from 90 to 35%); this is similar to the influence of increased concentrations of the shape-directing agent cetyltrimethylammonium bromide (CTAB) in industrial synthesis of gold particles.[21] Increased GSP concentrations also influenced the morphology of the nanoplates, favoring the morphogenesis of the triangular plates. Elucidation of the gene/protein sequence of GSP should help our understanding of its mechanism of action.

3.0. Nanoparticle synthesis *in vitro*

The examples mentioned above demonstrate the ability of organisms to synthesize a variety of materials under ambient conditions. From these examples, the components and conditions required for nanomaterial synthesis can be gleaned and used to inspire new ways of synthesizing particles *in vitro*. Researchers have taken advantage of the tailorability of biological molecules to establish new ways of synthesizing nanoparticles. These *in vitro* approaches have led to a better understanding of the relationships between the facilitating biomolecules, reaction conditions, and resultant nanomaterials. Here we provide examples of the ways in which peptides, proteins, viruses and polynucleotides are being utilized for nanoparticle synthesis *in vitro*.

3.1 Peptide-based synthesis

Like biomineralization proteins in nature, peptides provide an excellent biomimetic template for the controlled synthesis of different inorganic materials. They feature a rich chemical diversity ($-COO^-$, –SH, –OH and $-NH_2$ groups) of functional groups for metal binding, hydrophobic and hydrophilic amino acids, different secondary structures (random coil, α-helix, 3_{10}-helix, β-sheet) and biorecognition motifs. All of these features are encoded in the amino acid sequence and can contribute to biomineralization activity. Various peptide sequences have been used in the biomimetic synthesis of ceramic, metal sulfide, metal oxide and metallic nanoparticles with low polydispersity, good crystallinity, variable morphologies, and a wide range of biofunctionality under mild aqueous conditions. In the following, we will describe the

synthesis of inorganic materials using biomineralization-inspired and combinatorially-selected peptides, as well as the properties of the resulting material.

3.1.1 Biomineralization-inspired peptides. There have been numerous peptide-mediated approaches aimed at replicating the silica-precipitating activity of marine sponges and diatoms as well as controlling particle size and morphology.[4] At present, the R5 peptide (SSKKSGSYSGSKGSKRRIL) derived from a repeat unit of the *sil*1 gene from *Cylindrotheca fusiformis* diatoms remains the most popular biomimetic template for the synthesis of silica. Using the R5 peptide (polycationic and rich in –OH groups), spherical silica nanoparticles of 200 nm to several microns were synthesized *via* polycondensation of silicic acid (silicic acid is generated by the hydrolysis of precursor tetramethyl orthosilicate prior to addition of the peptide) in the presence of phosphate buffer. When subjected to chemical additives and external electrostatic or hydrodynamic fields, a fibrous network formed instead.[24] Silica morphology (spherical particles, fibrous structures, or hexagonal platelets) was dependent upon the template and its secondary structure; synthesis with mutant peptides of the R5 sequence,[25] a phage display peptide sequence of Si4-1 (MSPHPHPRHHHT),[24] and different molecular weight, conformation and handedness of poly-L-lysine (PLL), resulted in different structures.[25]

Silica precipitating templates were also utilized in the synthesis of non-natural metal oxides of titanium dioxide,[25] germanium oxide,[26] and gallium oxide.[25,27] For the synthesis of TiO_2, recombinantly expressed silaffin proteins induced the formation of nanocrystalline rutile at room temperature in the presence of titanium bis(ammonium lactato)dihydroxide (TiBALDH) precursors. Prior to this study, the synthesis of the rutile phase of TiO_2 had only been achieved at extreme acidic conditions or high temperatures (600 °C). In addition to TiO_2, amorphous GeO_2 was synthesized under ambient conditions and neutral pH using PLL, polyallylamine, or peptides derived by phage display. Under these conditions, particles precipitated *via* polyallylamine were spherical with sizes ranging from 400 nm to 3 μm by SEM and noncrystalline by XRD. To control morphology of particles synthesized, Patwardhan and Carlson introduced external shear during the course of the reaction and obtained elongated GeO_2 particles.[26]

Another example of peptides that are utilized for biomineralization *in vitro* are the cysteine-rich phytochelatins. In nature, these peptides, which are short repeating sequences of $(\gamma EC)_nG$, are expressed by plants, bacteria and fungi in response to high levels of environmental, toxic metal ions (Cd^{2+}, Hg^{2+}, Pb^{2+}). *In vivo*, phytochelatins sequester and detoxify Cd^{2+} ions, resulting in the biosynthesis of CdS nanoparticles. Labile cellular sulfide is also generated and incorporated into Cd-peptide complex to form less toxic CdS particles.[7] Consequently, a number of linear and dendritic peptides have been based on phytochelatins for the synthesis of CdS *in vitro*. Advantages of using peptides as stabilizing agents for the biomimetic synthesis of CdS include generation of smaller particle sizes with high quantum yields, increased stability in aqueous solutions, and resistance to oxidation. For example, Spoerke *et al*. used branched peptides rich in cysteine and aspartic acid in the presence of Cd^{2+} and Na_2S to produce many particle sizes of CdS with fluorescence emission ranging from 495 to 555 nm, as illustrated in Fig. 3;[28] Qian and co-workers used cysteine and mixed solvents in addition to a source of Cd^{2+} and S^{2-} to obtain different microstructures of CdS particles that consisted of urchin-like, polypod and nanowire structures.[29]

3.1.2 Peptides inspired by biological processes. The use of peptides for biomineralization *in vitro* extends beyond naturally-occuring peptides or derivatives of them. In some cases, biological processes and the biomolecules involved in them have inspired new synthesis methods as well. For instance, some amino acids, such as tryptophan and tyrosine

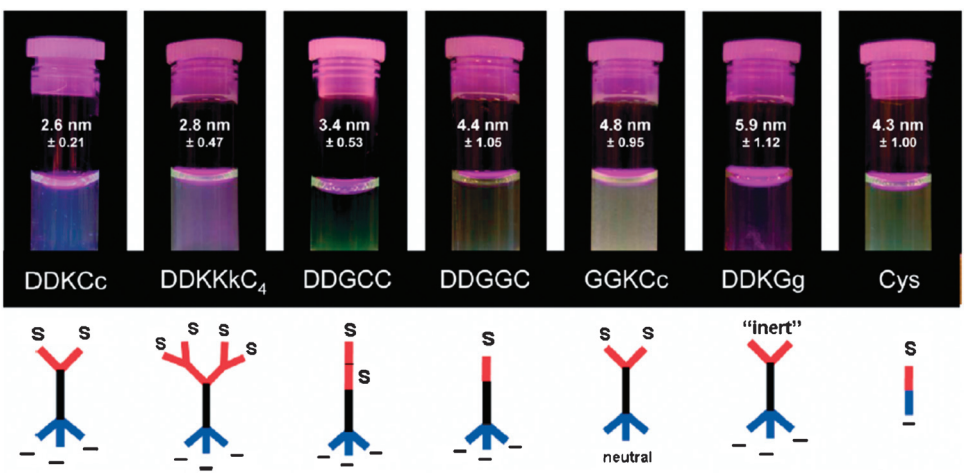

Fig. 3 (Top) Image of multiple sized CdS particles stabilized by different peptides, each exhibiting a different fluorescence emission. CdS particle sizes and peptide used for synthesis are included for each. (Bottom) Schematic representation of peptide structure; where (–) indicates carboxylate group of aspartic acid and (S) indicates thiol group of cysteine. E. D. Spoerke and J. A. Voigt, Influence of engineered peptides on the formation and properties of cadmium sulfide nanocrystals, *Adv. Funct. Mater*., 2007, **17**, 2031–2037. Copyright 2007, Wiley-VCH Verlag GmbH & Co. KGaA. Reproduced with permission.

form intermediates, protonated tryptophan and tyrosine radicals through resonance stabilization, which are involved in electron and hydrogen transport in biological systems.[30] Si and Mandal have exploited such intermediates for transferring electrons to metal ions to form metal nanoparticles. In a simple 'one-pot' process, they used a tripeptide ligand with a C-terminal tyrosine residue or C-terminal tryptophan residue for the formation of silver and gold nanoparticles.[30] In this case, the peptide sequence controlled the final nanoparticle properties, improving monodispersity, size and functionality of nanoparticles as compared to classical gold synthesis methods (citrate, alkanethiols).

3.1.3 Combinatorial peptide libraries for nanoparticle synthesis. While nature has perfected the biomineralization of certain materials by the implementation of highly specific biomolecules, the synthesis of other materials deemed non-essential by biological systems, such as high-temperature and non-oxide ceramics, is precluded by the lack of appropriate biomolecular templates in nature. An alternative solution involves using combinatorial approaches such as phage display peptide libraries (PD) or *E. coli* cell surface display (CSD) libraries to identify peptides from a pool of random sequences (10^7–10^{10}) that bind to inorganic targets and non-natural materials with high affinity.[31,32]

In both cases, 'panning' against inorganic targets involves incubating a library of bacteriophages (for PD) or bacterial cells (for CSD) with an inorganic substrate.[32] Each phage or bacterial cell displays on its surface a different peptide that may or may not bind to substrate. For PD, after incubation of the PD library with a desired target, the substrate is washed to remove unbound/non-specific phages and strongly bound phages are eluted by lowering pH. DNA from these tightly-bound phages is then sequenced to yield the amino acid sequence of the displayed peptide. Similarly, CSD peptide libraries are incubated with an inorganic substrate to promote binding of the bacterial cells to the inorganic surface through the displayed peptide, cycled through a growth phase, and then sequenced. In some cases, the resulting peptide sequences are then screened for biomineralization activity. It should be emphasized, however, that the use of these high affinity sequences does not necessarily mean they are capable of synthesizing and templating nanoparticles.

PD peptide libraries are the preferential method for rapidly identifying peptide templates for nanoparticle synthesis due to the complexity of cell surfaces when using CSD. As a result, PD has become increasingly widespread due to the prevalence of commercially available all-in-one phage display panning kits and improvements in phage display techniques.[24,31] Consequently, the depository of peptide sequences selective for different materials continues to ever-increase.

3.2 Protein templates for synthesis

3.2.1 Proteins as scaffolds. In contrast to peptides that have limited ability for spatial and structural control in three dimensions, as a group proteins possess unique architectures, surface chemistries, topologies, and confined cavities/cages to direct synthesis and nanoparticle growth. As a result, the physical dimensions and features of the template are preserved in the final nanoparticle product, *e.g.*, size, crystallinity and shape. For example, the size of an interior protein cavity can precisely govern the size of a resulting nanoparticle by acting as a constrained reaction vessel for synthesis. Size control is an attractive feature of protein-templated synthesis, and compared to other synthetic methodologies, produces nanoparticles with high monodispersities critical for catalysis, optics and electronics. In nature, the mammalian iron storage protein ferritin best exemplifies control over nanoparticle size as demonstrated by its ability to biomineralize 7 nm ferrihydrite particles. Ferritin also represents the first modified protein template to be used as a cage for the size-controlled, biomimetic synthesis of atypical inorganic nanoparticles (*e.g.*, Mn_3O_4, $Ni(OH)_3$, In_2O_3, CdS, Co_3O_4, ZnS) from a variety of different metal ion precursors.[33] Based on the successes using eukaryotic ferritin, Dps, a small ferritin analog from the bacterium *Listeria innocua*, has been reported for the synthesis of encapsulated CdS nanoparticles[34] and iron oxide catalysts for carbon nanotube growth.[35]

Besides the biomineralization of ferrihydrite by ferritin, most proteins do not function as biomineralization templates in nature but may possess other characteristics (*e.g.*, metal binding sites, negatively or positively charged interfaces, hydrophilic surfaces and unique geometries) that can be exploited for inorganic nanoparticle synthesis. Examples include enzymes and the protein capsid of viruses. To exploit these features, molecular biology is routinely used to genetically engineer these molecules for inorganic nanoparticle synthesis. Genetic modifications include the introduction of short peptide sequences known to synthesize and stabilize nanoparticles or substitution of a charged residue or metal binding site for a non-essential amino acid in the protein sequence. A crystal structure for the protein/capsid is helpful for this endeavor as it permits exact positioning of the engineered sites. The N- or C-terminus is the preferred location for mutations since in these locations the added residues often do not disrupt the tertiary fold of the protein and provide exposed binding domains. These modifications result in protein cavities or exterior surfaces that exhibit an affinity for a single metal ion. Interior cage modifications have included the introduction of a silver-reducing peptide AG4 within ferritin,[35] addition of a peptide sequence specific for the $L1_0$ phase of CoPt to the small heat shock protein from *Methanococcus jannaschii*.[33]

Among nanoparticle templates, viruses offer unique architectures and scaffolds, multiple protein capsids, self-assembling capability and high symmetry for synthesis.[33] Each of these enable control over a specific aspect of nanoparticle synthesis with respect to nanoparticle size, shape and organization. For example, the anisotropic shape of viruses has led to the synthesis of Au–Co_3O_4 nanowires as electrodes for lithium ion batteries, CoPt and FePt nanowires, ZnS–virus liquid crystals, polycrystalline CdS, and organized Au nanoparticles on the exterior of the viral capsid.[33,34,36] Conversely, the interior cavity space of the cowpea chlorotic mottle virus was used for the synthesis of paratungstate, decavanadate and iron oxide nanoparticles.[33]

3.2.2 Enzymatic synthesis of nanoparticles. Enzymes exemplify the potential to harness an unparalleled level of activity

and substrate specificity for nanoparticle synthesis. Of particular interest is the redox activity and presence of oxidizable amino acids (*e.g.*, thiol group of cysteine) in enzymes for the reduction of metal ions to metal nanoparticles. For instance, the native enzyme α-amylase served as a substrate to Au nanoparticles *via* oxidation of the free and exposed S–H groups.[37] It not only reduced $AuCl_4^-$, but also imparted enzymatic activity to nanoparticles even after reduction as observed by a zone of clearance in a starch agar plate test. In contrast to the direct reduction of gold ions, enzymes were indirectly used to synthesize gold nanoparticles as a means to monitor activity. For example, hydrogen peroxide produced as a by-product from the oxidation of glucose to gluconic acid by glucose oxidase was used as a reducing agent in the catalytic deposition of Au on Au. Similarly, tyrosinase, alkaline phosphastase and acetylcholinesterase were reported to promote gold nanoparticle formation by reduction of Au^{3+} *via* generation of L-Dopa from tyrosine and the hydrolysis products of *p*-aminophenol and thiocholine, respectively.[38]

3.3 DNA/RNA for nanoparticle synthesis

Until recently, DNA and RNA have primarily been reported for the assembly of many inorganic nanoparticles and heterostructures through hybridization of complementary single-stranded DNAs functionalized with particles, and Mg^{2+}-dependent RNA–RNA interactions.[39] As a result, the use of DNA or RNA for synthesis is limited to only a few reports. For synthesis, the phosphate backbone and purine/pyrimidine bases of DNA and RNA have a high affinity for metal ions, similar to that of certain amino acid residues in peptides (histidine, lysine, aspartic acid); RNA also exhibits catalytic activity in the formation of metal–metal bonds. These features, in addition to programmable biomolecule shapes (hairpins and loops, RNA ladders, circular DNA plasmids, linear DNA oligonucleotides), sizes (few bases to 10 000 bases), and sequences, are considerably appealing for synthesis. Eaton and colleagues first reported the formation of hexagonal palladium nanoparticles using RNA selected from a library of $\sim 10^{14}$ sequences and the metal precursor complex of dibenzylideneacetone palladium(0).[40] Later, RNA from yeast was used to synthesize fcc PbS quantum dots with high quantum efficiencies that emitted at 675 nm.[41] Using DNA, infrared emitting PbS nanocrystals with an emission shifted to ~1100 nm were obtained with a single nucleotide of guanidine triphosphate[42] or 20 kilobase DNA chain.[43] With the latter, PbS nanocrystals were stable in aqueous solutions and blood plasma for extended periods of time. The DNA template directs the growth of PbS through Pb^{2+} binding at the phosphate backbone and stabilizes the surface through interactions with the purine and pyrimidine bases.

4.0. Applications

4.1 Quantum dots

Quantum dots are nm-sized semi-conducting crystals with unique quantum optical properties due to their ability to confine electron hole pairs (excitons) on a nm-scale. The properties of quantum dots (high quantum yield, low photobleaching) have inspired the synthesis of many novel hybrid structures for light harvesting and photoactivated catalysis,[44] innovations in sensing/labeling/bioimaging,[45] and improvements in nanoelectronics and nanophotonics.[46] In the case of light harvesting, single-walled carbon nanotube–CdS composites were capable of generating moderate photocurrent levels from visible light irradiation with extremely high efficiencies.[47] Also, CdS particles have been successfully interfaced with an assortment of enzymes to yield quantum dot–enzyme hybrid complexes. In each case, an electron generated in the conduction band of CdS upon excitation is directly transferred to the active center of the bound enzyme and used in the reduction of the substrate or carbon nanotube matrix. The use of quantum dots has a significant advantage over the chemical means of enzyme activation: *i.e.*, the ability to turn enzyme activity on or off by controlling illumination of quantum dots. For example, excitation of CdS–cytochrome P450[44] enzyme hybrids resulted in the hydroxylation of myristic acid to α- and β-hydroxymyristic acid products *via* activation of P450 enzyme by superoxide and hydroxyl radicals generated from quantum dot excitation. Alternatively, cytochrome P450 was substituted with hydrogenase and activated by quantum dots for the photoproduction of hydrogen as illustrated in Fig. 4.[48] Recently, Ohtani and co-workers loaded a silica-coated CdS particle with rhodium for the photoreduction of nitrobenzene to azoxybenzene.[49] In this

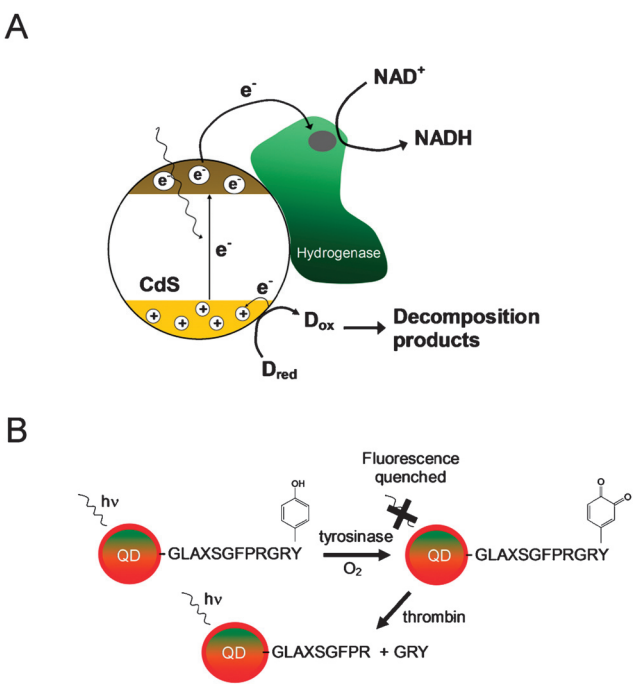

Fig. 4 (A) Photoproduction of hydrogen by CdS-hydrogenase complex. Light generates an exciton in CdS, an electron is transferred to active center of hydrogenase, protons are reduced to hydrogen by enzyme through NADH path, and formate back donates an electron to CdS to fill the hole. (B) Detection of enzyme activity using peptide conjugated quantum dots. Tyrosinase oxidizes the tyrosine residue of peptide conjugated quantum dots to a quinone, resulting in quenching of quantum dot fluorescence. Upon addition of thrombin, which selectively cleaves the GRY sequence, the quantum dot regains its original fluorescence.

case, rhodium was used as a cocatalyst in place of an enzyme to effectively capture photogenerated electrons from CdS. Upon irradiation for 24 h, rhodium loaded CdS particles resulted in a 68% product yield.

Biofunctionalized quantum dots have also garnered attention as reporter agents for following enzymatic reactions.[50] Banin and colleagues engineered a CdSe–ZnS-peptide conjugate that possessed a peptide (GLAXSGFPRGRY) with an exposed tyrosine residue and a thrombin recognition site for monitoring tyrosinase and thrombin hydrolytic activity, respectively, by means of fluorescence (Fig. 4). In the presence of tyrosinase, the C-terminal tyrosine residue of the peptide was transformed into L-Dopa and oxidized into an *o*-quinone group. Interaction of the *o*-quinone-modified tyrosine with the QD induced fluorescence quenching by 45%. In addition to containing a tyrosine, the functionalized peptide was designed to include a proteolytic site (GRY) cleavable by thrombin. Addition of thrombin to QD–peptide resulted in hydrolytic cleavage of the GRY peptide segment and recovery of the QD fluorescence.

4.2 Biofunctionalized gold nanoparticles

Gold nanoparticles provide a catalytically active metallic surface; if coated with a biomolecule, they obtain an alternate source of functionality much like an enzyme. In an elegant example of enzyme-like structure and behavior, Scrimin and colleagues demonstrated that multiple copies of peptides assembled on a gold nanoparticle surface form a functional catalytic subunit with enzyme-like activity for the hydrolysis of 2,4-dinitrophenylbutyrate.[51] This was achieved by including four catalytically active residues (histidine, two arginines and lysine) in the peptide. These residues acted as a nucleophile, general acid, and/or general base, exploiting cooperativity between different groups of adjacent peptides at the catalytic site imparted by nanoparticle surface, and creation of a localized water-free environment similar to an enzyme. Notably, the activity of the nanozyme was modulated by the amount of substrate present.[51]

Bio-functionalized gold nanoparticles serve as reconfigurable sensing platforms by utilizing the biomolecular recognition of functionalized biomolecules with the unique colorimetric, conductive and SERS (surface enhanced raman scattering) properties of gold. For example, gold nanoparticles can be reconfigured to sense many different analytes by simply changing the peptide or DNA sequence with which they are functionalized. In terms of detecting recognition of the analyte, colorimetric assays are attractive for their simplicity, sensitivity and spectrum of visible color changes in response to the aggregation or dispersion of gold particles upon target binding. As a result, color changes are accompanied by either a red or blue shift depending on the nanoparticle system. To date, colorimetric assays involving gold nanoparticles have been developed for the detection of a variety of targets including bacterial toxins, enzyme activity, and as a means to probe pH, protein conformation, and level of eukaryotic gene expression[52,30]. For metal ion sensing, DNA-functionalized particles and mercaptopropionic acid-derivatized gold separately detected Hg^{2+} ions at a concentration of 100 nM by monitoring changes in the melting point transition of oligonucleotides bound with metal ions or shifts in the plasmon resonance. Colorimetric assays have also been developed for the detection of cholera toxin by the aggregation of lactose-stabilized gold particles at a target concentration of 54 nM.[52]

The SERS of gold and silver nanoparticles is another effective means to detect binding of targets. Unlike colorimetric or conductivity based detection techniques, SERS spectroscopy offers the ability to detect near-single molecule coupled with the unique spectroscopic fingerprints of targets. In one of the first nanoparticle-based, Raman detection schemes for biomolecules, Mirkin and colleagues demonstrated the detection of oligonucleotide sequences from several viral genes using gold nanoparticle probes functionalized with oligonucleotide recognition sequences, labeled with Raman-active dyes, and enhanced *via* silver.[53] The addition of a distinct Raman-active dye for each target significantly reduced the complexity of spectra arising from similar oligonucleotide targets; silver enhancement was necessary to achieve a strong SERS signal. Other targets detected using gold and silver nanoparticle probes included protein–small molecule binding, protein–protein interactions, bacteria and pollen.

4.3 Silica nanoparticles

The ability to synthesize nanoparticles at ambient conditions makes them appealing for applications such as enzyme encapsulation. Biomineralized silica, in particular, is an excellent platform for enzyme encapsulation due to the porosity of silica nanoparticles produced through biomineralization. When enzymes are added during nanoparticle synthesis, they are often entrapped inside the particle. The applications of entrapped enzymes are numerous and include biosensors, decontamination systems, immobilized enzyme reactors and biocatalysis.[54] Indeed, enzymes such as butyrylcholinesterase, catalase and horseradish peroxidase have been successfully entrapped inside silica nanoparticles that were synthesized with the R5 peptide.[54,55] For butyrylcholinesterase, this method of enzyme entrapment immobilized 90% of the enzyme activity from the precursor solution and retained 100% of its activity; 220 mg of enzyme could be loaded per gram of silica (20% w/w). This loading efficiency was in contrast to that of sol–gel methods of enzyme entrapment in silica, in which less than 10% of initial enzyme activity is entrapped, and where loading was restricted to 0.1–5% w/w.[54] In addition, entrapment in biomineralized silica preserved the stability of butyrylcholinesterase during storage, desiccation and exposure to high temperatures. To demonstrate direct application of the silica-encapsulated enzyme, the particles were utilized in a liquid chromatography column as a fluidized-bed and packed-bed flow-through 'reactors'. Under these conditions, the enzymes maintained excellent stability; complete conversion of substrate persisted for over 1000 column volumes in the fluidized bed system, and for over 2000 column volumes in the packed bed system.

For a different application, Naik *et al*. co-entrapped catalase with magnetic CoPt or a streptavidin-conjugated quantum dots (CdSe@ZnS), providing the enzyme-loaded silica particles with enhanced functionality.[55] The magnetic properties of

the CoPt incorporated into the particle allowed the particles to be separated from solution with a magnet, resulting in an easy means by which to reuse the entrapped enzyme. The quantum dot-loaded nanoparticles exhibited emission spectra equivalent to control quantum dots when excited at the appropriate wavelength, allowing their detection in solution.

5.0. Conclusions

Bacteria, fungi, algae, plants and animals have evolved to biomineralize a variety of substances, for specific purposes and as by-products of cellular pathways. Much has been learned about the specific biomolecules, substrates, cell machinery and reaction conditions required for biomineralization. These lessons have been applied to the exploration of *in vitro* methods of mineral synthesis. In some cases, the natural biomolecules, or versions of them, have been used *in vitro*. In other cases, nature's ability to synthesize minerals has inspired researchers to search for bio-templates for creating materials that, to our knowledge, are not synthesized by organisms. These combined approaches have resulted in a plethora of new, bio-derived synthesis methods for producing a variety of materials for use in nanotechnology. Notably, most of these methods allow 'one-pot' syntheses under ambient conditions. The future success of bio-directed synthesis of nanomaterials relies on researchers' ability to tailor the size, structure, properties and uniformity of the materials, and to deposit the materials onto small-scale, next-generation sensors and devices.

References

1 E. Bauerlein, in *Handbook of Biomineralization*, ed. E. Bauerlein, Wiley-VCH Verlag GmbH & Co., Weinheim, 2007, ch. 1, pp. 1–14.
2 N. Kröger and N. Poulsen, in *Handbook of Biomineralization*, ed. E. Bauerlein, Wiley-VCH Verlag GmbH & Co., Weinheim, 2007, ch. 3, pp. 43–57.
3 M. Hildebrand, *J. Nanosci. Nanotechnol.*, 2005, **5**, 1–12.
4 J. C. Weaver and D. E. Morse, *Microsc. Res. Tech.*, 2003, **62**, 356–367, and references therein.
5 D. Schüler and R. B. Frankel, *Appl. Microbiol. Biotechnol.*, 1999, **52**, 464–473, and references therein.
6 A. Komeili, *Annu. Rev. Biochem.*, 2007, **76**, 351–366.
7 J. M. Slocik, M. R. Knecht and D. W. Wright, in *Encyclopedia of Inorganic Chemistry*, ed. R. B. King, John Wiley and Sons, New York, 2nd edn, 2005, pp. 371–391.
8 N. Poulsen and N. Kröger, *J. Biol. Chem.*, 2004, **279**, 42993–42999, and references therein.
9 L. G. Frigeri, T. R. Radabaugh, P. A. Haynes and M. Hildebrand, *Mol. Cell. Proteomics*, 2006, **5**, 182–193.
10 W. E. G. Müller, A. Boreiko, U. Schlossmacher, X. Wang, M. N. Tahir, W. Tremel, D. Brandt, J. A. Kaandorp and H. C. Schröder, *Biomaterials*, 2007, **28**, 4501–4511, and references therein.
11 H. C. Schröder, A. Boreiko, M. Korzhev, M. N. Tahir, W. Tremel, C. Eckert, H. Ushijima, I. M. Müller and W. E. G. Müller, *J. Biol. Chem.*, 2006, **281**, 12001–12009.
12 T. Coradin and P. J. Lopez, *ChemBioChem*, 2003, **4**, 251–259.
13 M. J. Uriz, X. Turon, M. A. Becerro and G. Agell, *Microsc. Res. Tech.*, 2003, **62**, 279–299.
14 D. Schüler and R. B. Frankel, *Appl. Microbiol. Biotechnol.*, 1999, **52**, 464–473, and references therein.
15 T. Matsunaga, T. Suzuki, M. Tanaka and A. Arakaki, *Trends Biotechnol.*, 2007, **25**, 182–188, and references therein.
16 A. Komeili, *Annu. Rev. Biochem.*, 2007, **76**, 351–366, and references therein.
17 D. Faivre, L. H. Bottger, B. F. Matzanke and D. Schuler, *Angew. Chem., Int. Ed.*, 2007, **46**, 8495–8499.
18 A. Arakaki, J. Webb and T. Matsunaga, *J. Biol. Chem.*, 2003, **278**, 8745–8750.
19 X.-Z. Li, H. Nikaido and K. E. Williams, *J. Bacteriol.*, 1997, **179**, 6127–6132.
20 N. Hu and B. Zhao, *FEMS Microbiol. Lett.*, 2007, **267**, 17–22.
21 J. Xie, J. Y. Lee, D. I. C. Wang and Y. P. Ting, *Small*, 2007, **3**, 672–682.
22 B. Nair and T. Pradeep, *Cryst. Growth Des.*, 2002, **2**, 293–298.
23 R. Y. Sweeney, C. Mao, X. Gao, J. L. Burt, A. M. Belcher, G. Georgiou and B. L. Iverson, *Chem. Biol.*, 2004, **11**, 1553–1559.
24 R. R. Naik, S. E. Jones, C. J. Murray, J. C. McAuliffe, R. A. Vaia and M. O. Stone, *Adv. Funct. Mater.*, 2004, **14**, 25–30, and references therein.
25 S. L. Sewell and D. W. Wright, *Chem. Mater.*, 2006, **18**, 3108–3113.
26 S. V. Patwardhan and S. J. Clarson, *Polymer*, 2005, **46**, 4474–4479.
27 D. Kisailus, J. H. Choi, J. C. Weaver, W. Yang and D. E. Morse, *Adv. Mater.*, 2005, **17**, 314–318.
28 E. D. Spoerke and J. A. Voigt, *Adv. Funct. Mater.*, 2007, **17**, 2031–2037.
29 S. Xiong, B. Xi, C. Wang, G. Zou, L. Fei, W. Wang and Y. Qian, *Chem.–Eur. J.*, 2007, **13**, 3076–3081.
30 S. Si and T. K. Mandal, *Chem.–Eur. J.*, 2007, **13**, 3160–3168, and references therein.
31 U. Kirplani and B. K. Kay, *Curr. Opin. Biotechnol.*, 2005, **16**, 470–475, and references therein.
32 M. Sarikaya, C. Tamerler, A. K.-Y. Jen, K. Schulten and F. Baneyx, *Nat. Mater.*, 2003, **2**, 577–585, and references therein.
33 M. Uchida, M. T. Klem, M. Allen, P. Suci, M. Flenniken, E. Gillitzer, Z. Varpness, L. O. Liepold, M. Young and T. Douglas, *Adv. Mater.*, 2007, **19**, 1025–1042, and references therein.
34 K. Iwahori, T. Enomoto, H. Furusho, A. Miura, K. Nishio, Y. Mishima and I. Yamashita, *Chem. Mater.*, 2007, **19**, 3105–3111.
35 R. M. Kramer, L. A. Sowards, M. J. Pender, M. O. Stone and R. R. Naik, *Langmuir*, 2005, **21**, 8466–8470, and references therein.
36 K. T. Nam, D.-W. Kim, P. J. Yoo, C.-Y. Chiang, N. Meethong, P. T. Hammond, Y.-M. Chiang and A. M. Belcher, *Science*, 2006, **312**, 885–888, and references therein.
37 A. Rangnekar, T. K. Sarma, A. K. Singh, J. Deka, A. Ramesh and A. Chattopadhyay, *Langmuir*, 2007, **23**, 5700–5706.
38 I. Willner, R. Baron and B. Willner, *Adv. Mater.*, 2006, **18**, 1109–1120.
39 J. M. Slocik and R. R. Naik, *Curr. Nanosci.*, 2007, **3**, 117–120, and references therein.
40 L. A. Gugliotti, D. L. Feldheim and B. E. Eaton, *Science*, 2004, **304**, 850–852.
41 A. Kumar and A. Jakhmola, *Langmuir*, 2007, **23**, 2915–2918.
42 S. Hinds, B. J. Taft, L. Levina, V. Sukhovatkin, C. J. Dooley, M. D. Roy, D. MacNeil, E. H. Sargent and S. O. Kelley, *J. Am. Chem. Soc.*, 2006, **128**, 64–65.
43 L. Levina, V. Sukhovatkin, S. Musikhin, S. Cauchi, R. Nisman, D. P. Bazett-Jones and E. H. Sargent, *Adv. Mater.*, 2005, **17**, 1854–1857.
44 B. I. Ipe and C. M. Niemeyer, *Angew. Chem., Int. Ed.*, 2005, **44**, 1–5.
45 E. L. Bentzen, F. House, T. J. Utley, J. E. Crowe, Jr and D. W. Wright, *Nano Lett.*, 2005, **5**, 591–595.
46 D. V. Talapin and C. B. Murray, *Science*, 2005, **310**, 86–89.
47 I. Robel, B. A. Bunker and P. V. Kamat, *Adv. Mater.*, 2005, **17**, 2459.
48 A. I. Nedoluzhko, I. A. Shumilin and V. V. Nikandrov, *J. Phys. Chem.*, 1996, **100**, 17544–17550.
49 B. Pal, T. Torimoto, K.-I. Okazaki and B. Ohtani, *Chem. Commun.*, 2007, 483–485.
50 R. Gill, R. Freeman, J.-P. Xu, I. Willner, S. Winograd, I. Shweky and U. Banin, *J. Am. Chem. Soc.*, 2006, **128**, 15376–15377.
51 P. Pengo, L. Baltzer, L. Pasquato and P. Scrimin, *Angew. Chem., Int. Ed.*, 2007, **46**, 400–404.
52 C. L. Schofield, R. A. Field and D. A. Russell, *Anal. Chem.*, 2007, **79**, 1356–1361, and references therein.
53 Y. C. Cao, R. Jin and C. A. Mirkin, *Science*, 2002, **297**, 1536–1539.
54 H. R. Luckarift, J. C. Spain, R. R. Naik and M. O. Stone, *Nat. Biotechnol.*, 2004, **22**, 211–213.
55 R. R. Naik, M. M. Tomczak, H. R. Luckarift, J. C. Spain and M. O. Stone, *Chem. Commun.*, 2004, 1684–1685.

